Journal of Evolving Space Activities
Vol. 1, Article No. 17, 2023
DOI: 10.57350/jesa.17

Function Test of Experimental System to Obtain Laser Ignition Characteristics of Low-Temperature Boron/Potassium Nitrate

By Kohei MATSUI,[1)] Yoshiki MATSUURA,[2)] Shinichiro TOKUDOME[3)] and Koki KITAGAWA[1)]

[1)]*Department of Space Systems Engineering, Kyushu Institute of Technology, Kitakyushu, Japan*
[2)] *Technologies Development Department, IHI Aerospace Co., Ltd., Tomioka, Japan*
[3)] *Institute of Space and Astronautical Science, Japan Aerospace Exploration Agency, Sagamihara, Japan*

(Received August 30th, 2022)

In order to use laser ignition systems for solid rocket motors operating in deep space environments, it is necessary to elucidate the laser ignition characteristics of the ignition charge in low-temperature environments. This study aims to design an experimental system that can confirm the ignition threshold, ignition delay, and ignition temperature by irradiating an ignition charge with a diode laser in a low-temperature environment. Ignition experiments at room temperature were conducted. The data were evaluated statistically to obtain an ignition threshold with the maximum likelihood method. The relationship between the laser irradiation duration and the laser power with respect to the ignition threshold was obtained. The target value of the low-temperature environment temperature was determined as -50 °C. We examined the requirements of the experimental system and conceptually designed the system to simulate the low-temperature environment. It was confirmed that the constructed experimental system cooled the ignition charge to -50 °C. In the ignition experiment, the ignition charge was successfully ignited at room temperature and at low temperature. The ignition delay, the ignition temperature, and the high-speed image were obtained. Eventually, the validity of the experimental system was confirmed through the function tests.

Key Words: Laser Ignition, B/KNO_3, Laser Diode, Low-Temperature Environment, Solid Rocket

1. Introduction

For the ignition of a solid rocket, a small combustor called an igniter is used. The igniter is loaded with an ignition charge. The ignition charge burns first, then the propellant in the igniter burns and the flame from the igniter ignites the propellant of the solid rocket motor. Conventionally, the electric ignition method has been used to ignite the igniter. In the electric ignition method, a resistor is embedded in the igniter, and the ignition is performed by Joule heating generated by applying electric current to the resistor. In this method, there is a risk of unexpected ignition due to electrical disturbances such as static electricity, lightning, and radio waves. A heavy device for safety control, such as a safe-and-arm device, is required. Therefore, a laser ignition system has been proposed as an alternative to the conventional electric ignition system. In the laser ignition system, the ignition is performed by irradiating a laser directly onto the ignition charge. Since the laser can concentrate high energy, the ignition capability is high, and the ignition charge does not need to be sensitive. Moreover, since the ignition charge is irradiated directly, conductors such as wires do not come into the igniter, and there is no risk of malfunction due to electrical disturbance. Because of the above, the laser ignition system is expected to simplify the structure of the igniter and improve safety.[1)] With the recent miniaturization of semiconductor lasers, laser ignition systems are being considered as ignition systems for rocket motors. In addition, a laser ignition system has been adopted for the solid-rocket motor of a micro spacecraft that will carry out a lunar landing mission[2)]. It is considered that the laser ignition system will be used for deep-space missions. In order to use the laser ignition system practically, it is necessary to improve reliability the same as or more than the electric ignition systems currently in use. As the ignition charge of the laser ignition system, boron potassium nitrate (B/KNO_3) is chosen, because B/KNO_3 is the igniter of a lot of actual solid rockets. In addition, by using most part of the existing igniter, a developed ignition system has high reliability, and the development cost can be reduced.

Our goal is to realize the laser ignition system in deep space environment. It is necessary to clarify the mechanism of laser ignition of B/KNO_3 to design the system. Previous studies on the laser ignition of B/KNO_3 have been done by different research groups. Koizumi et al. clarified the laser ignition characteristics of B/KNO_3 in vacuum at a room temperature, which is essential for the application to the propellant of spacecraft rocket[3)]. Nakayama et al. performed one-dimensional numerical calculations considering the temperature dependence of thermophysical properties[4)]. They showed that the experimental values of ignition temperature and ignition delay were close to the calculated values under room temperature, atmospheric pressure, and one-dimensional conditions. Ahmad et al. studied the effect of wavelength on the ignition delay time of several energetic materials including B/KNO_3[5)]. Sivan et al. showed the effect of boron particle size on the ignition delay[6)]. Although there have been many studies on laser ignition of B/KNO_3 at room temperature as described above, the mechanism at low temperature has not been clarified. Since deep space is low-temperature environment, it is necessary to obtain the laser ignition characteristics of the B/KNO_3 in the low temperature state. First of all, development

of an experimental system that can obtain laser ignition characteristics at low temperature is necessary.

The purpose of this study is to develop the experimental system and method for investigating the ignition threshold, ignition delay, and ignition temperature with a semiconductor laser in a low-temperature environment. As a first step, we constructed an experimental system that can investigate the ignition threshold of the ignition charge at room temperature, and construct and validate a method to statistically obtain ignition threshold of ignition charge. The relationship between the laser irradiation duration and laser power to the ignition threshold were obtained. As a second step, based on the results, the experimental system for laser ignition of ignition charge in the low-temperature environment was constructed. Then, we performed a function confirmation experiment to confirm that the requirements were satisfied.

2. Ignition Threshold Experiments at Room Temperature

2.1. Experimental system

Figure 1 shows a schematic diagram of the experimental system at room temperature and atmospheric pressure. B/KNO_3 pellets manufactured by NiGK Corporation were used as the ignition charge. The wight fraction are 28% for B, 70 % for KNO_3, and 2 % for binder. The dimensions and mass are Φ3.2 mm × 2.0 mm and 30.0 mg ± 2.9 mg, respectively. In this ignition experiment, the ignition charge was ignited in a fume hood because the ignition charge produces toxic combustion gas. The laser is a laser diode manufactured by Unitac, with a wavelength of 440 nm and a maximum laser output of 2.5 W. The laser was configured to irradiate the bottom of the ignition charge through the optical fiber, and an acrylic plate with a thickness of 0.20 mm ± 0.05 mm was installed between the optical fiber and the ignition charge so that the optical fiber was not damaged by the combustion gas of the ignition charge. The optical fiber was a core diameter of 200 μm, NA 0.22, and multi-mode. Since the laser irradiation damages the acrylic plate, the plate was replaced after laser irradiation regardless of

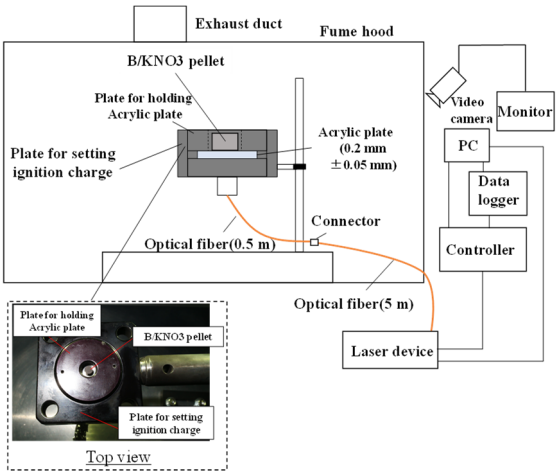

Fig. 1. Schematic diagram of the experimental system at room temperature.

ignition or non-ignition. The distance between the acrylic plate and the tip of the fiber was adjusted to 0.02-0.03 mm with the shim. The ignition was observed with a video camera, and ignition or non-ignition was confirmed. The laser power is changed by setting the electric current. The relationship between the laser power and the electric current is linear on average. However, the laser device has significant deviation of power. Therefore, the laser power is measured before and after each ignition test.

2.2. Experimental method

Two types of experiments were performed: a simple experiment to obtain ignition threshold and an experiment to obtain ignition threshold with the maximum likelihood method. In the simple experiment to obtain ignition thresholds, the approximate ignition threshold was obtained. The ignition threshold was estimated simply to guarantee the validity and determine the initial value of the experiments to obtain the ignition threshold with the maximum likelihood method. In the simple experiment, four trials were carried out. First, the ignition experiment was conducted with the electric current value of the laser diode at an appropriate value near the ignition/ non-ignition boundary. In the case of non-ignition at the first trial, the electric current value is increased by 0.04 A at the second trial. In the case of ignition, the electric current value is decreased by 0.04 A. Next, the ignition experiment with the current value in the middle of the first and second trials was conducted. Finally, the ignition experiment was conducted with the value between the ignition and non-ignition electric current values of two of these three. With this, the boundary between ignition and non-ignition was observed with an accuracy of 0.01 A.

The experiment to obtain the ignition threshold with the maximum likelihood method was conducted by changing the irradiation duration and laser power to evaluate the experimental system and method. The initial value was determined from the approximate ignition threshold obtained from the simple experiment to obtain the ignition threshold. The experiments were conducted based on the Up and Down method.[3] The Japanese Defense Agency standard,[4] recommends that the number of experiments was 15 or more. We carried out the experiment using 25 samples, which is more than recommended number.

We conducted the maximum likelihood analysis as follows. The ignition probability $X(P_i)$ for a laser power P_i was assumed as a cumulative normal distribution function,

$$X(P_i) = \int_{-\infty}^{P_i} \frac{1}{\sqrt{2\pi}\sigma} \exp\left(-\frac{u-\mu}{2\sigma^2}\right) du \,. \quad (1)$$

μ and σ express the average and the standard deviation of the cumulative normal distribution function, respectively. The probability of non-ignition is expressed as $1 - X(P_i)$. For example, the probability $L(\mu, \sigma)$ that events ignition, non-ignition, and ignition in three trials is

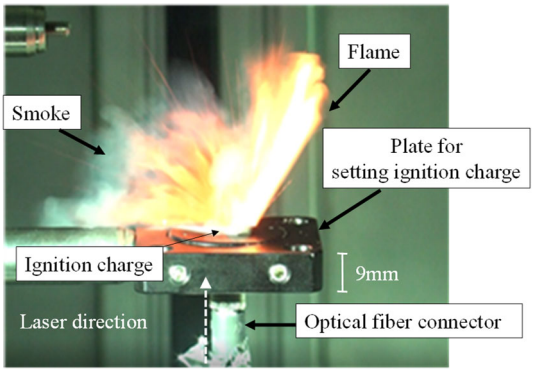

Fig. 2. View immediately after the ignition of B/KNO_3 ignition charge (Laser power: 0.82 W, irradiation duration: 10 ms).

$$L(\mu,\sigma) = X(P_1)\cdot\left(1-X(P_2)\right)\cdot X(P_3) = \left\{\int_{-\infty}^{P_1}\frac{1}{\sqrt{2\pi}\sigma}\exp\left(-\frac{(u-\mu)^2}{2\sigma^2}\right)du\right\} \left\{1-\int_{-\infty}^{P_2}\frac{1}{\sqrt{2\pi}\sigma}\exp\left(-\frac{(u-\mu)^2}{2\sigma^2}\right)du\right\} \left\{\int_{-\infty}^{P_3}\frac{1}{\sqrt{2\pi}\sigma}\exp\left(-\frac{(u-\mu)^2}{2\sigma^2}\right)du\right\}. \quad (2)$$

The specific values of $(\hat{\mu},\hat{\sigma})$ that maximize $L(\mu,\sigma)$ are the maximum likelihood estimated value.

The simple experiments to obtain ignition threshold were conducted with laser irradiation durations of 5, 10,15, 100, 200, 500, and 1000 ms. The experiments to obtain ignition threshold with the maximum likelihood method were conducted with laser irradiation durations of 5, 25, 100, 1000 ms. It was expected that there would be a point where the ignition threshold does not change even after long-term irradiation due to the equilibrium between the heat input from the laser and the heat loss such as thermal diffusion, heat transfer to the acrylic plate, and radiation.

2.3. Experimental results

Figure 2 shows a view which is captured by the video camera immediately after the ignition of B/KNO_3 ignition charge. When ignited, it burned out in less than a second with flames and smoke. As an example of the results of the simple experiment to obtain ignition threshold, table 1 shows the ignition/non-ignition and laser power of the experiment at an irradiation duration of 15 ms. In this result, the boundary between ignition and non-ignition was between the set electric current values of 0.55A and 0.54 A, and the average laser power was 268.5 mW, which is the average of the irradiation

Table 1. Ignition/non-ignition and laser power of simple experiment to obtain the ignition threshold at irradiation duration of 15 ms (○: ignition, ×: non-ignition. Values in parentheses indicate the laser power, mw).

No.	Electric Current, A				
	0.54	0.55	0.56	0.57	0.58
1	× (263.0)				
2					○(300.9)
3			○(282.7)		
4		○(274.0)			

Table 2. Ignition/non-ignition and laser power of experiment to obtain ignition threshold with maximum likelihood method at irradiation duration of 25 ms (○: ignition, ×: non-ignition. Values in parentheses indicate the laser power, mw).[2)]

No.	Electric Current, A				
	0.54	0.55	0.56	0.57	0.58
1					○(216.6)
2				○(212.6)	
3			○(198.1)		
4		×(187.7)			
5			○(195.6)		
6		×(186.6)			
7			○(196.8)		
8		×(186.3)			
9			×(194.7)		
10				×(205.0)	
11					○(212.6)
12				×(204.5)	
13					○(212.5)
14				○(209.4)	
15			○(196.8)		
16		○(186.1)			
17	×(177.2)				
18		×(184.4)			
19			×(192.4)		
20				○(206.9)	
21			×(195.2)		
22				○(205.2)	
23			○(194.4)		
24		×(185.8)			
25			×(192.9)		

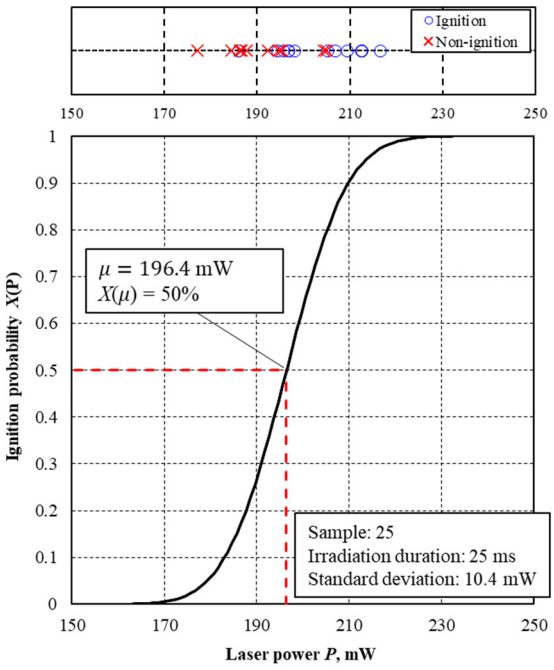

Fig. 3. The ignition probability drawn using values by the maximum likelihood estimation method and results of ignition/non-ignition.

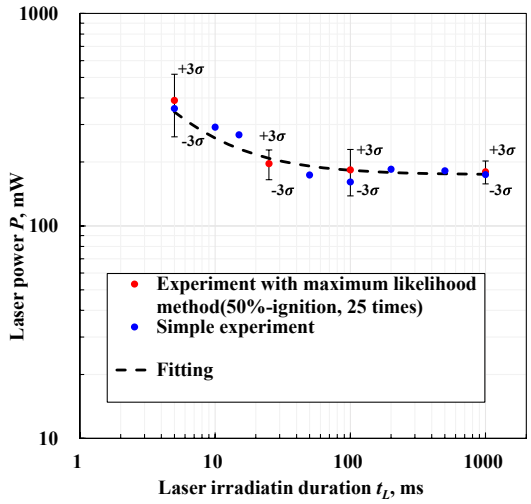

Fig. 4. Relationship between the laser irradiation duration and the laser power with respect to the ignition threshold obtained in the simple experiments to obtain ignition threshold and the experiments to obtain ignition threshold with maximum likelihood method.[2)]

powers of 274.0 mW and 263.0 mW, respectively.

As an example of the experiments to obtain ignition threshold with the maximum likelihood method, table 2 shows the ignition/non-ignition and laser power of the ignition experiments at an irradiation duration of 25 ms. The ignition probability drawn by using the maximum likelihood estimated value is shown in Fig. 3. The upper graph in Fig. 3 shows the results of ignition/non-ignition. In this result, the average laser power and standard deviation values were 196.4 mW and 10.4 mW, respectively.

Figure 4 shows the relationship between the laser irradiation duration and the laser power with respect to the ignition threshold obtained in the simple experiments to obtain the ignition threshold and the experiments to obtain ignition threshold with maximum likelihood method. The blue dots show the data of the simple experiments to obtain ignition threshold, and the red dot shows the data of the experiments to obtain ignition threshold with maximum likelihood method. The laser power required for ignition decreases as the irradiation duration increases. The simple obtained data fluctuates with probability, but it should be within the range of ± 3σ obtained from the experiments to obtain ignition threshold with maximum likelihood method. Since all the simply obtained data from Fig. 4 are within ± 3σ, it can be considered that the way of the experiments to obtain ignition threshold with maximum likelihood method is appropriate.

2.4. Statistical analysis of ignition threshold

The maximum likelihood estimated values $(\hat{\mu}, \hat{\sigma})$ include an errors. In order to calculate the ignition probability appropriately, the error should be considered. The graph examples of the error in the parameter of ignition probability are shown in Fig. 5. The average value represents the laser power with 50% ignition probability and has the error as shown in Fig. 5 (a). The standard deviation is the laser power that

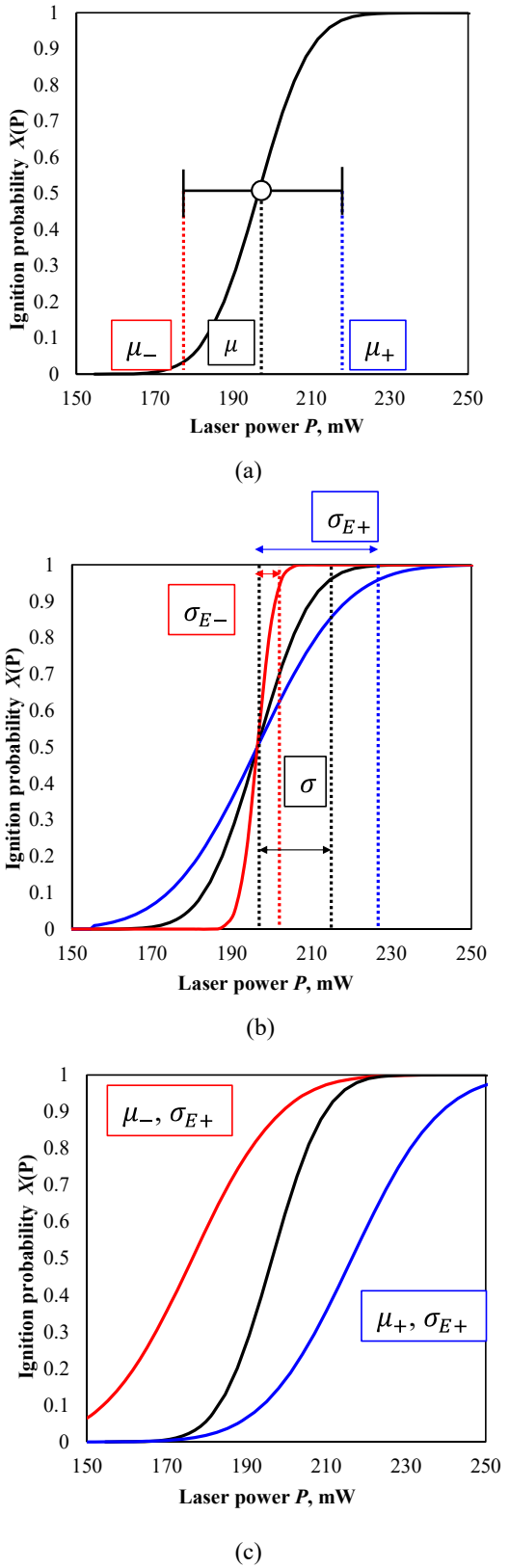

Fig. 5. Graph examples of the error in the parameter of ignition probability. (a) Error of the average. (b) Error of the standard deviation. (c) Ignition probability curve to obtain upper limit and lower limit.

Table 3. 95% confidence interval of averages of ignition probability at each irradiation duration.

Irradiation duration, ms	Laser power, mW		
t_L	$\hat{\mu}$	μ_+	μ_-
5	390.2	407.7	372.7
25	196.4	200.7	192.1
100	183.1	189.3	176.9
1000	179.9	183.0	176.8

represents the spread of the probability distribution, and the error affects the slope of the probability curve as shown in Fig. 5 (b). The upper limit of average and the lower limit of standard deviation are used to obtain the upper limit of ignition probability. On the other hand, the lower limit of average and the upper limit of standard deviation are used to obtain the lower limit of ignition probability, as shown in Fig. 5(c).

Here, the average value and standard deviation were tested, and then the laser power of the ignition probabilities of 0.0001% and 99.9999% were calculated with a confidence interval of 95 %. The t-tests for the average value and the χ^2-test for the standard deviation were conducted. First, the average value was evaluated. μ was the average value of the true ignition probabilities of the ignition charge, that is, the population average, and define the t-statistic as follows.

$$t = \frac{\hat{\mu}-\mu}{\sqrt{\sigma^2/n}} , \tag{3}$$

Since the t-statistic follows the t-distribution, the confidence interval can be expressed as

$$\left[\hat{\mu} - t_{\frac{\alpha}{2}}\frac{\sigma}{\sqrt{n}}, \hat{\mu} + t_{\frac{\alpha}{2}}\frac{\sigma}{\sqrt{n}}\right] . \tag{4}$$

Here, n is the number of trials, and the degree of freedom of t distribution is $n - 1 = 24$. α is the probability that μ is not included in the confidence interval, and here we calculated the 95% confidence interval. Therefore, $\alpha = 0.05$. Table 3 shows the results of calculating the average upper confidence threshold μ_+ and the average lower confidence threshold μ_- using $t_{0.025}(24) = 2.064$. Next, the standard deviation σ was evaluated. When the variance of the true ignition probability of ignition charge, that is, the population variance, is σ_E^2,

Table 4. 95% confidence interval of standard deviations of ignition probability at each irradiation duration.

Irradiation duration, ms	Laser power, mW		
t_L	σ	σ_{E+}	σ_{E-}
5	42.4	59.0	33.1
25	10.4	14.5	8.1
100	15.1	21.0	11.8
1000	7.4	10.3	5.8

$$\chi^2 = (n-1)\frac{\sigma^2}{\sigma_E^2} , \tag{5}$$

follows the χ^2-distribution. At this time, the confidence interval can be expressed as

$$\left[\frac{(n-1)\sigma^2}{\chi^2_{\frac{\alpha}{2}}}, \frac{(n-1)\sigma^2}{\chi^2_{1-\frac{\alpha}{2}}}\right] . \tag{6}$$

The 95% confidence interval of σ was calculated in the same way as μ. Table 4 shows the results of calculating the standard deviation upper confidence threshold σ_{E+} and the standard deviation lower confidence threshold σ_{E-} using $\chi^2_{0.025}(24) = 39.4$ and $\chi^2_{0.975}(24) = 12.4$.

The laser powers with ignition probabilities of 0.0001% and 99.9999% were estimated using the average value and standard deviation at the confidence level of 95% obtained above. The probabilities of 0.0001% and 99.9999% in the cumulative normal distribution were given by ± 4.753 σ, respectively. For the standard deviation, the upper confidence threshold value σ_{E+} was used. The average values were calculated using the lower confidence threshold value μ_- for 0.0001% and the upper confidence threshold value μ_+ for 99.9999%. The calculated

Table 5. Laser power with 0.0001% and 99.9999% probability of ignition at 95% confidence interval.

Irradiation duration, ms	Laser power, mW	
t_L	probability of ignition 0.0001% $\mu_- - 4.753\sigma_{E+}$	probability of ignition 99.9999% $\mu_+ + 4.753\sigma_{E+}$
5	92.3	688.1
25	123.3	269.5
100	77.0	289.2
1000	127.9	231.9

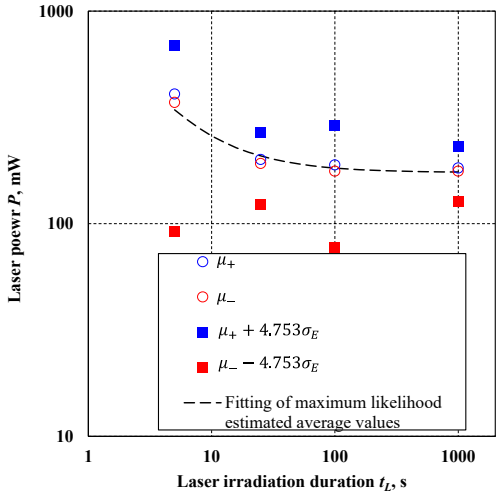

Fig. 6. Relationship between the laser irradiation duration and the laser power with respect to the ignition threshold.

ignition thresholds are shown in Table 5. Figure 6 shows the relationship between the laser irradiation duration and the laser power with respect to the ignition threshold. The dashed curve is fitting line obtained in Fig. 4.

From these results, it was confirmed that a statistically reliable ignition threshold could be obtained using the experimental results of the Up and Down method. In addition, we were able to calculate values that could be sufficiently operated and designed with 25 trials. It was confirmed that the ignition / non-ignition of the ignition charges at room temperature could be obtained, and the relationship between the laser irradiation duration and the laser power with respect to the ignition threshold can be obtained by using the experimental apparatus we developed, the experimental method, and the statistical processing method used in this study. Therefore, it was judged that a laser ignition experimental system in a low-temperature environment could be constructed based on the same experimental system and method.

3. Laser Ignition Experimental System for Ignition Charges at Low Temperature

3.1. Requirements for the experimental system

3.1.1. Low-temperature environment

In order to clarify the low-temperature environment simulated by the experimental apparatus, it is necessary to examine the temperature of the spacecraft in deep space. We considered a spacecraft observing Jupiter and the temperature of the spacecraft. The spacecraft is assumed to be a simple cylinder, and the surface material is chrome plated. Chromium plating has a large value of absorption rate with respect to radiation and can keep the spacecraft at a high temperature. It is thought that the higher the temperature of the spacecraft, the easier it is for the onboard equipment to operate and for the ignition charge to ignite. Equation (5) shows the state in which the amount of solar heat input to the spacecraft and the amount of heat radiation from the spacecraft to outer space are in equilibrium. It was assumed that the spacecraft is made of a material with good thermal conductivity (metal, etc.) and has a uniform temperature.

$$\alpha_S A' P = \varepsilon_H \beta A T^4 \quad . \tag{7}$$

Here, α_S: Sunlight absorption rate on the surface of the spacecraft, A' [m^2]: Sunlight irradiation cross-sectional area, P: Solar energy, ε_H: Emissivity from the surface of the spacecraft, β [W/(m^2 · K^4)]: Stefan-Boltzmann constant, A [m^2]: Surface area of the spacecraft, T: Spacecraft temperature (K). Defining that the diameter of a spacecraft, which is a simple cylinder, is R [m] and the length is L [m], A' and A can be written as Eqs. (8) and (9), respectively.

$$A' = R \times L \quad , \tag{8}$$

$$A = R \times \pi \times L \quad . \tag{9}$$

By transforming Eq. (5) and substituting Eqs. (8) and (9), Eq. (10) is leaded as follows.

$$\begin{aligned} T &= \left(\frac{\alpha_S}{\varepsilon_H}\right)^{\frac{1}{4}} \left(\frac{A' P}{\sigma A}\right)^{\frac{1}{4}} \\ &= \left(\frac{\alpha_S}{\varepsilon_H}\right)^{\frac{1}{4}} \left(\frac{R \times L \times P}{\sigma \times R \times \pi \times L}\right)^{\frac{1}{4}} \\ &= \left(\frac{\alpha_S}{\varepsilon_H}\right)^{\frac{1}{4}} \left(\frac{P}{\sigma \pi}\right)^{\frac{1}{4}} \quad . \end{aligned} \tag{10}$$

Solar energy decreases toward the deeper universe, and the power is approximately inversely proportional to the square of the distance. When flying near Jupiter, the solar energy P becomes Eq. (11). Hence, the solar energy of the earth P_E is 1353 W/m^2, and the distance of Jupiter D_J is 5.2 AU.

$$\begin{aligned} P = P_E \times \left(\frac{1}{D_J}\right)^2 &= 1353 \times \left(\frac{1}{5.2}\right)^2 \\ &= 50.0 \text{ W/m}^2 \quad . \end{aligned} \tag{11}$$

For chrome plating, α_S = 0.45, εH = 0.05 are assumed. These are measurement reference values by space-related manufacturers. The temperature can be obtained from Eq. (10), as shown below,

$$\begin{aligned} T &= \left(\frac{0.45}{0.05}\right)^{\frac{1}{4}} \left(\frac{R \times L \times 50.0}{5.67 \times 10^{-8} \times R \times \pi \times L}\right)^{\frac{1}{4}} \\ &= 224 \text{ K} \\ &= -49 \text{ °C}. \end{aligned} \tag{12}$$

Based on this, the spacecraft flying near Jupiter is calculated to be about -50 °C, so this is set as the target value for the low-temperature environment temperature simulated by the experimental system.

3.1.2. Other requirements

- The ignition charge is cooled to -50 °C.
- The ignition charge is prevented from frost and dew formation.
- The optical system such as the lens and optical fiber is not polluted by the combustion gas of the ignition charge and must be used multiple times.
- The ignition / non-ignition of the ignition charge is observed.
- The laser power, the ignition temperature of the laser irradiation surface, and the ignition delay is measured.
- The laser beam is focused on the surface of the ignition charge.
- The profile of the laser intensity distribution can be measured.

3.2. Ignition experiment system at low temperature

Figure 7 shows a schematic of the experimental system at low temperatures. A cooler manufactured by Nihon Blower is used as the cooling device. This uses a Peltier device for the cooling plate, and can make a low-temperature environment of -50° C. This cooling plate cools the ignition charge with the ignition charge installation plate made of copper. The ignition charge installation plate has a hole of Φ3.4 mm x 2.0 mm in the center to install the ignition charge. This is the size that the

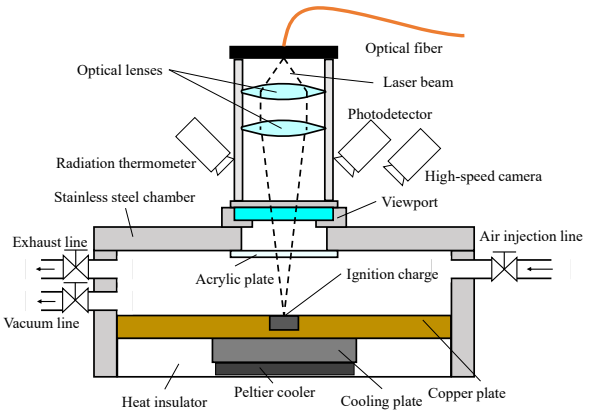

Fig. 7. Schematic of the experimental system at low temperature.

B/KNO_3 pellets. This cooling device is equipped with a thermocouple to measure the temperature of the cooling plate. Also, another thermocouple is equipped on the surface of the ignition charge to measure the temperature in order to confirm that the ignition charge is cooled to -50 °C. This thermocouple detaches from the surface of the ignition charge when the ignition experiment. Frost and dew condensation on the surface of the ignition charge are prevented by covering the ignition charge installation plate with a container and making a vacuum. The pressure vessel that can withstand a vacuum is manufactured using stainless steel. The laser beam is emitted from the optical fiber and focused with two lenses. The beam is irradiated through the glass viewport and the acrylic plate. The acrylic plate is installed between the viewport and the ignition charge to prevent the lens from pollution by the combustion gas when the ignition charge is ignited. The acrylic plate is replaced every time after laser irradiation regardless of ignition / non-ignition because it is damaged by the laser irradiation. The laser power is controlled by changing the electric current value applied to the laser diode. The relationship between the laser irradiation duration and the laser power with respect to the ignition threshold is obtained. The high-speed camera and the radiation thermometer observe the ignition charge surface through the viewport. The ignition / non-ignition and ignition delay of the ignition charge are obtained with a high-speed camera. The photodetector also obtains the ignition delay by measuring the luminescence from the combustion. The radiation thermometer measures the temperature of the ignition charge surface at the ignition. The measurable temperature range is 220-2000 °C. To measure the temperature, the emissivity must be taken into account, so it was assumed to be a black body and set to 1.

The laser diode is the same as in the experiments at room temperature, described in section 2.1. The wavelength is 440 nm, and the maximum laser output is 2.5 W. The beam diameter at the surface of the ignition charge is controlled by adjusting the distance between the two lenses. The laser intensity changes by controlling the beam diameter and laser power. The laser intensity profile at the surface of the ignition can be measured by adjusting the distance between the optics and the profiler. The optical fiber has a core diameter of 200 μm, an NA of 0.22, and is multi-mode.

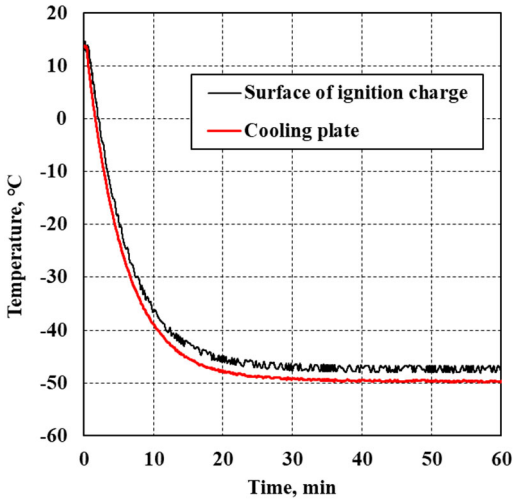

Fig. 8. History of temperatures of the surface of ignition charge and the cooling plate.

4. Function Confirmation Tests

4.1. Cooling performance of the experimental system

Before the ignition experiment, the temperature of the ignition charge should be cooled to -50 °C. We confirmed the ignition charge could be cooled appropriately by comparing the temperature of the ignition charge with that of the cooling plate. Figure 8 shows the temperature history of the surface of the ignition charge and the cooling plate. The initial time in Fig. 8 represents the time when cooling is started. Both temperatures decreased to -40° C in 10 minutes, and almost -50 ° C in 30 minutes. The temperature of the ignition charge is slightly higher than that of the cooling plate. After 30 minutes, both temperatures are constant. Based on the results of this test, we

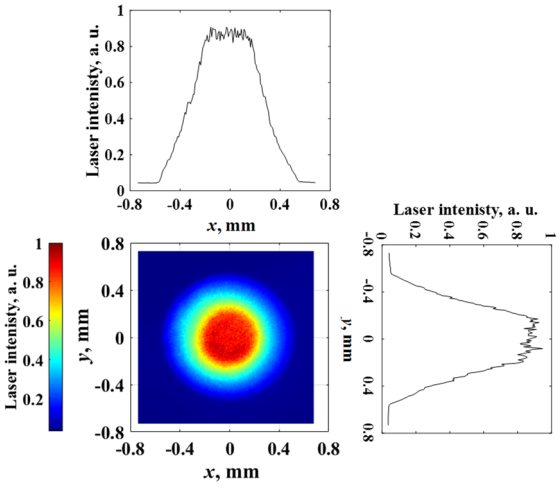

Fig. 9. Beam profile of 2D image and intensity distributions of *x* and *y* directions at the center of the beam

cooled the ignition charge for 30 minutes before laser irradiation in the ignition experiment.

4.2. Beam profile at surface of ignition charge

The laser beam profile was measured with a 2D CCD beam profiler. The focal lengths of the collimator lens and focusing lens are 25 mm and 75 mm, respectively. The distance between the beam profiler and the viewport was adjusted using a height gauge and a linear stage. The beam profile is measured through the viewport. The measurement result at the focal point is shown in Fig. 9. The figure shows the 2D contour and intensity distributions of *x* and *y* directions at the center of the beam. The laser intensity is presented as arbitrary units. The beam profile has the top-hat intensity distribution. The laser beam diameter was calculated according to the definition of D86 width. The D86 width is defined as the diameter of the circle containing 86 % of the laser power and calculated as 0.68 mm. The intensity distribution is assumed to be similar regardless of the laser power.

4.3. Ignition experiment at room temperature and low temperatures

An ignition experiment was conducted at room temperature and at low temperature to confirm that the ignition charge was ignited. The result is shown in Table. 6. In the experiment, laser irradiation duration was set to 1000 ms. The temperatures of the ignition charge in this experiment were almost 15 ° C at room temperature and -48 ° C at low temperature. The ignition
charge could be ignited at both temperatures. The ignition thresholds are assumed to exist between results of ignition/non-ignition. The boundary at room temperature is between 0.80 A and 0.85 A, while that at low temperature is between 0.85 A and 0.90 A. These results showed that the ignition charge at each temperature was ignited with the same level of the power. However, the difference between both results was not so clear. Only three experiments were conducted at each temperature, the number of trials is not enough to discuss the difference in the ignition threshold between room temperature and low temperature quantitatively. In the future, statistical tests are necessary to evaluate the ignition threshold appropriately, as explained in section 2.3.

4.4. Measurement results with photodetector, radiation thermometer, and high-speed camera

An ignition experiment was conducted to confirm that ignition delays, ignition temperatures, and high-speed images of the ignition charge surface could be obtained. The irradiation duration is 1000 ms, and the irradiation power is 703 mW. The measurement result with the photodetector is shown in Fig. 10. The signal was 0 V before the laser beam is irradiated, then it was about 3 V during the irradiation. The first signal rise from 3 V is regarded as the ignition delay, which was 0.737 s. We consider that the signal is disturbed after the first rise because the smoke from the combusted ignition charge interfered with the emission from the ignition charge surface. However, since this is a post-ignition behavior, there is no problem in detecting the ignition delay. We confirmed that the photodetector could acquire the ignition delay.

Table 6. Ignition/non-ignition with room temperature and low temperature. (〇: ignition, ×: non-ignition. Values in parentheses indicate the laser power, mW and temperature,° C).[2)]

Electric current, A	Ignition/Non-ignition	
	Room temperature	Low temperature
0.90	〇(498.1 mW, 15.1 °C)	〇(488.0 mW, -48.1 °C)
0.85	〇(457.6 mW, 15.6 °C)	×(443.1 mW, -48.1 °C)
0.80	×(426.0 mW, 15.0°C)	×(419.1 mW, -48.3 °C)

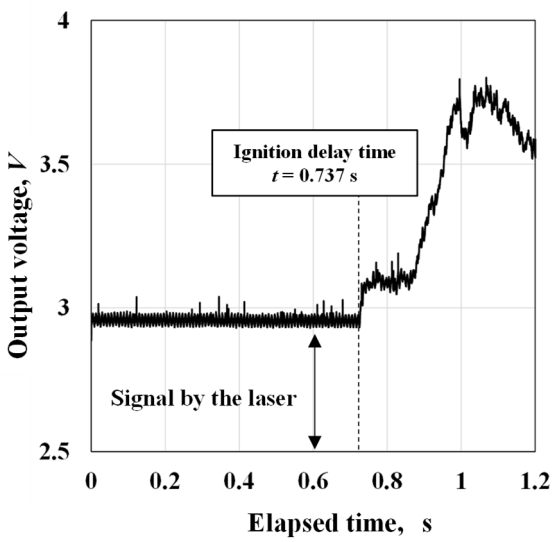

Fig. 10. The output of the photodetector and elapsed time of the laser irradiation

The measurement result with the radiation thermometer is shown in Fig. 11. The measurement range is more than 220 °C, and the temperature was measured from approximately 0.4

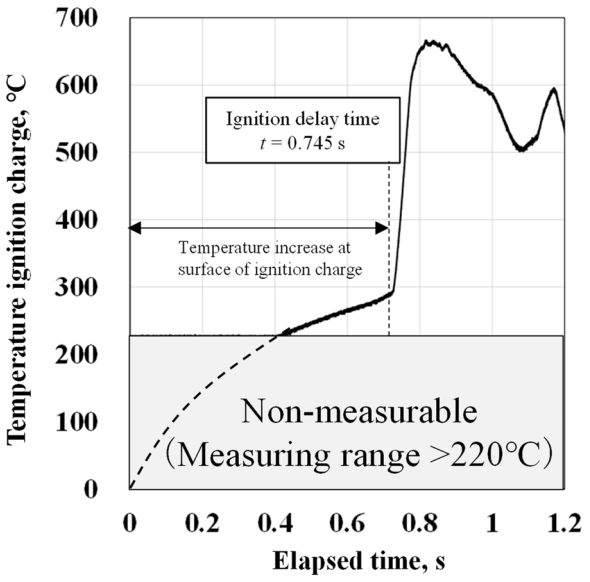

Fig. 11. The temperature of the ignition charge and elapsed time of the laser irradiation

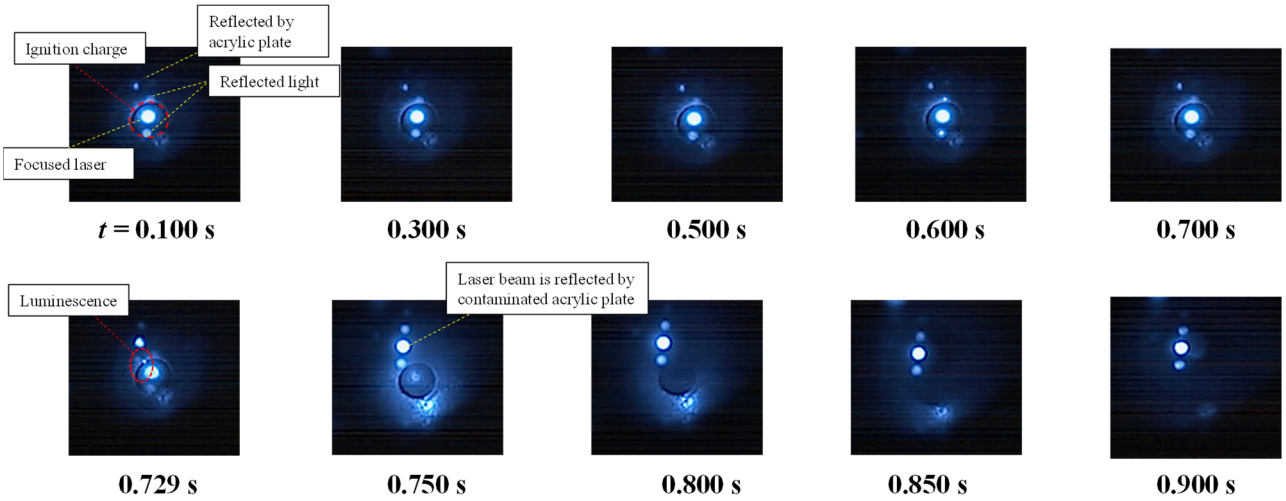

Fig. 12. High-speed images of the surface of the ignition charge during laser irradiation

seconds after the start of laser irradiation. The broken line in the figure shows the image of the temperature increase. There is a moment of rapid temperature increase at a certain time, which is considered as the ignition delay time and is 0.745 s. Similar to the measurement result with the photodetector, the signal is disturbed after a rapid temperature rise. Since this is a post-ignition phenomenon, this does not affect the temperature measurement. The ignition temperature is defined as the temperature at which it begins to rise rapidly. The ignition temperature is 293 °C. This value is lower than that in the previous study[3] (about 450 °C). This may be because the radiation from the ignition charge was measured through the acrylic plate, and radiation intensity was attenuated. In addition, the ignition charge was assumed to be a blackbody which caused the low ignition temperature. In the future, the ignition charge's emissivity and the acrylic plate's transmittance should be considered for calibration.

The images measured by the high-speed camera are shown in Fig. 12. The circular line in the center of each image indicates the shape of the ignition charge surface. The value below the images indicates the time from the start of laser irradiation. The frame rate was 10000 fps. The laser beam is focused on the surface of the ignition charge, and the reflected light is seen near the focused laser. The reflected light by acrylic plate also can be seen in the figure. The surface of the ignition charge did not change significantly during the first 0.7 seconds of the laser irradiation. A luminous emission was observed 0.729 seconds after the start of the laser irradiation, and this time was considered as the ignition. The picture after the ignition shows that the smoke blocked the laser beam. The amount of smoke increases which shows the combustion reaction is progressing. The smoke seems to interfere with the emission from the ignition charge, as explained for Fig. 12. The ignition delay was almost the same for the photodetector, radiation thermometer, and high-speed camera, confirming that the ignition delay could be obtained with each measurement device. Through function confirmation tests, the validity of the experimental apparatus was confirmed.

5. Conclusion

The followings were conducted for the purpose of developing an experimental system that can obtain the ignition threshold, ignition delay, and ignition temperature by heating the ignition charges with a laser diode in a low-temperature environment.

Experiments to obtain the ignition threshold at room temperature were conducted, and data for evaluating the ignition threshold were obtained. We conducted a statistical evaluation of the ignition threshold. It was confirmed that the relationship between the laser irradiation duration and the laser power with respect to the ignition threshold could be obtained.

The target temperature at a low-temperature environment was determined as -50 °C, which is estimated based on the spacecraft flying in Jupiter's orbit. We considered the requirements of the experimental system and designed the experimental system that simulates a low-temperature environment. Then, the function confirmation test was conducted to confirm that the requirements were satisfied. The test result shows the ignition charge was properly cooled to about -50 °C. The laser beam profile at the surface of the ignition charge was measured. The ignition experiments at room temperature and at low temperature were conducted, and it was confirmed that the ignition charge could be ignited in both environments, and the region where the threshold existed could be estimated. We also confirmed that a photodetector could acquire ignition delay, a radiation thermometer can acquire ignition temperature, and a high-speed camera can acquire high-speed images of the ignition charge surface. The validity of the experimental apparatus was confirmed through the function confirmation tests.

In the future, we plan to obtain laser ignition characteristics using the constructed experimental system and to construct the numerical calculation model to elucidate the ignition mechanism at low temperatures.

Acknowledgments

This research is supported by JAXA-Kyushu Institute of Technology joint research “Study on ignition limit of ignition charges with laser ignition” and IHI Aerospace-Kyushu Institute of Technology joint research “Survey on ignition limit in solid rocket ignition system using laser” and JSPS KENHI Grant Number 22K14425. We would like to express our gratitude here.

References

1) Minami, K., Matsuura, Y., Kitagawa, K., Arakawa S., Morishita, N., Takemae, T., Iwabuchi, S., Wada, A., and Tokudome, S.: Development Results of Laser Ignition System for Solid Rocket Motor, *TRANSACTIONS OF THE JAPAN SOCIETY FOR AERONAUTICAL AND SPACE SCIENCES, AEROSPACE TECHNOLOGY JAPAN*, 2021, **19 (2021)**, pp. 807-811.
2) Morishita, N., Sago, Y., Watanabe, K., Sasayama, H., Ike, Y., Hayakawa, A., et al.: Development of a laser ignition system for a solid rocket motor on the OMOTENASHI spacecraft, *Sci. Tech. Energetic Materials*, **83** (2022), pp. 59-64.
3) Koizumi. H., et al.: Study on laser ignition of boron / potassium nitrate in vacuum, *Sci. Tech. Energetic Materials*,**67** (2006), pp. 193-198.
4) Nakayama. H, Miyashita, T., Yoshitake, N., and Orita, R.: A numerical model of laser−induced ignition of boron / potassium nitrate pyrotechnic incorporating temperature dependence of thermophysical properties, *Sci. Tech. Energetic Materials*, . **71** (2010), pp. 98-105.
5) Ahmad, S. R, Russell, D. A., Leach. C. J.: Studies into Laser Ignition of Unconfined Propellants, *Propellants Explos., Pyrotech*., **26 (**2001), pp. 235–245.
6) Ahmad, S. R, and Russell, D. A.: Studies into Laser Ignition of Confined Pyrotechnics, *Propellants Explos., Pyrotech*., **33 (**2008), pp. 396 – 402.
7) Sivan, J, Haas, Y., Grinstein, D., Kochav, S., Kalontarov, L. : Boron particle size effect on B/KNO3 ignition by a diode laser, *Combustion and Flame*, **162 (**2015), pp. 516-527.
8) Matsui, K., Matsuura, Y., Arakawa, S., and Kitagawa, K.: Experimental evaluation of B/KNO_3 ignition limit for determining the specifications of laser ignition for solid rockets, *65th Space Sciences and Technology Conference*, Online, 2F02, 2021 (in Japanese).
9) Dixon, W. J., Mood, A. M. : A Method for Obtaining and Analyzing Sensitivity Data, *Journal of the American Statistical Association*, **43 (**1948), pp. 109-126.
10) National Defense Standards, NDS-Y7531, 2006 (in Japanese).